Stochastic heating in non-equilibrium plasmas

J. Vranjes

Von Karman Institute, Brussels, Belgium

Workshop on Partially Ionized Plasmas in Astrophysics, Tenerife
June 19-22, 2012

Outline

Outline

Space: observed properties (solar wind; solar atmosphere)

- Heating in general (chromosphere, corona, solar wind).
- Temperature anisotropy $[T_\perp > T_\parallel,\ T_\perp < T_\parallel]$.
- Dominant heating in the high-energy tail.
- Dominant bulk plasma heating.
- Dominant heating of ions; heavy ions better heated than light ones.
- Dominant heating of electrons.
- Transport (perpendicular to the magnetic field vector).
- Acceleration of particles $\cdots$

Some waves of interest (multi-component theory)

- Plasma (Langmuir) wave.
- Ion acoustic wave (IA, $\omega > \Omega_i$, $\omega < \Omega_i$).
- Ion cyclotron wave (IC).
- Electron cyclotron.
- Ion-Bernstein wave (IB).
- Lower-hybrid wave (LH).
- Upper-hybrid (UH).
- Oblique and transverse drift (OD, TD) wave.
- Standing wave (various waves).

Some features of stochastic heating

- Mostly electrostatic phenomena.
- Necessity for a large enough electric field; yet linear theory valid.
  - For (high frequency, $\omega > \Omega_i$) IA wave:

$$ek_z^2\phi|J_l(k_\perp\rho_i)|/m_i \geq \frac{\Omega_i^2}{16}, \quad l = 0, \pm 1, \pm 2 \cdots$$

-Heating in the high-energy tail of the ion distribution.

  - For IC and LH wave:

$$\frac{E}{B_0} > \frac{1}{4}\left(\frac{\Omega_i}{\omega}\right)^{1/3}\frac{\omega}{k_\perp}.$$

-Heating of the bulk and tail plasma.

- For OD wave:

$$k_y^2 \rho_i^2 \frac{e\phi}{\kappa T_i} \geq 1.$$

-Heating of bulk plasma.
-Better heating of heavier ions.
-Dominant perpendicular heating.

- For TD wave (essentially electromagnetic mode!):

$$\frac{k_\perp^2 E_{z1}^2}{\omega^2 B_0^2} > 1.$$

-Acceleration $\Rightarrow$ heating and transport.
-Acting on both ions and electrons.

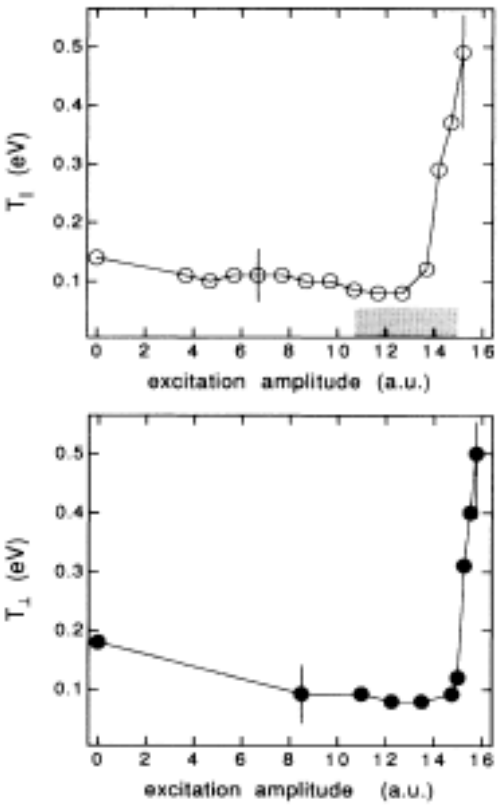

FIG. 2. Parallel (top) and perpendicular (bottom) ion temperatures vs wave excitation amplitude. f=25 kHz. These measurements, as well as those reported in the following graphs, have been taken a few cm downstream with respect to the antenna.

- Heating at ion-cyclotron harmonics.
- A. Fasoli *et al.*, Phys. Rev. Lett. **70**, 303 (1993).

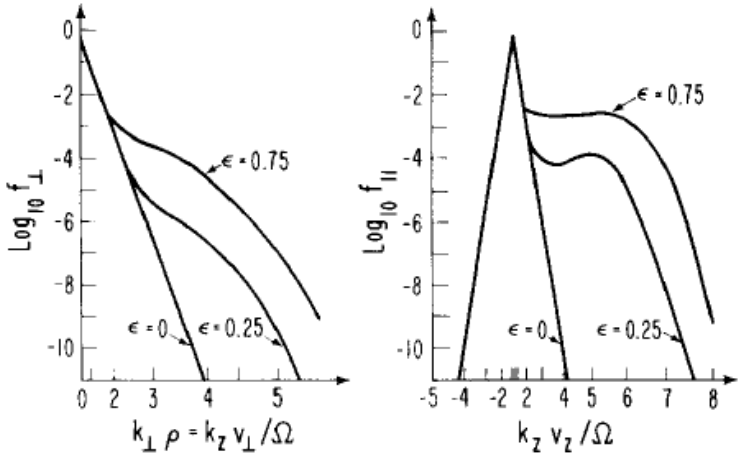

FIG. 9. The perpendicular ($f_\perp$) and parallel ($f_\parallel$) distribution functions in the presence of a finite-amplitude obliquely propagating, electrostatic wave. The distortions to Maxwellian distributions ($\epsilon = 0$) are shown for two wave amplitudes, $\epsilon = 0.25$ and 0.75.

- Stochastic tail heating by IA wave.
- Rapid process, rate comparable to gyro-frequency Ω.
- G. R. Smith and A. N. Kaufman, Phys. Fluids **21**, 2230 (1978).

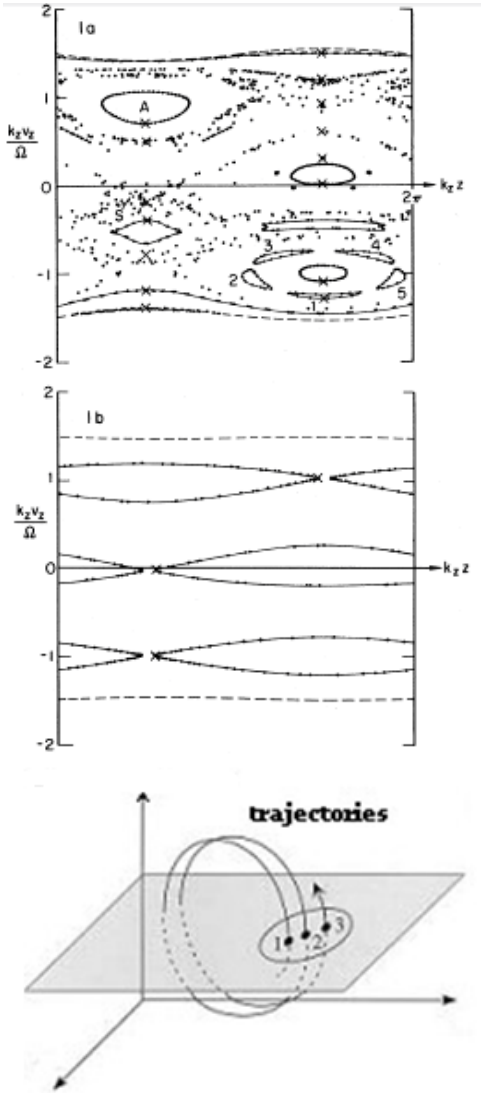

- IA wave: overlapping of resonances $\Rightarrow$ diffusion (loss of memory of initial conditions) .
- $\omega - k_z v_{Ti} = \pm l\Omega_i$.
  $\Rightarrow v_z = (\omega \pm l\Omega_i)/k_z$.
- High frequency IA mode $\omega > \Omega_i$.
- v_z finite for $k_z \neq 0$.
- Obliquely propagating with respect to $\vec{B}_0$!
- not large amplitude $n_1/n_0 \sim 0.1$.
- G. R. Smith and A. N. Kaufman, Phys. Rev. Lett. **70**, 303 (1993).

Drift-Alfvén wave heating in tokamak

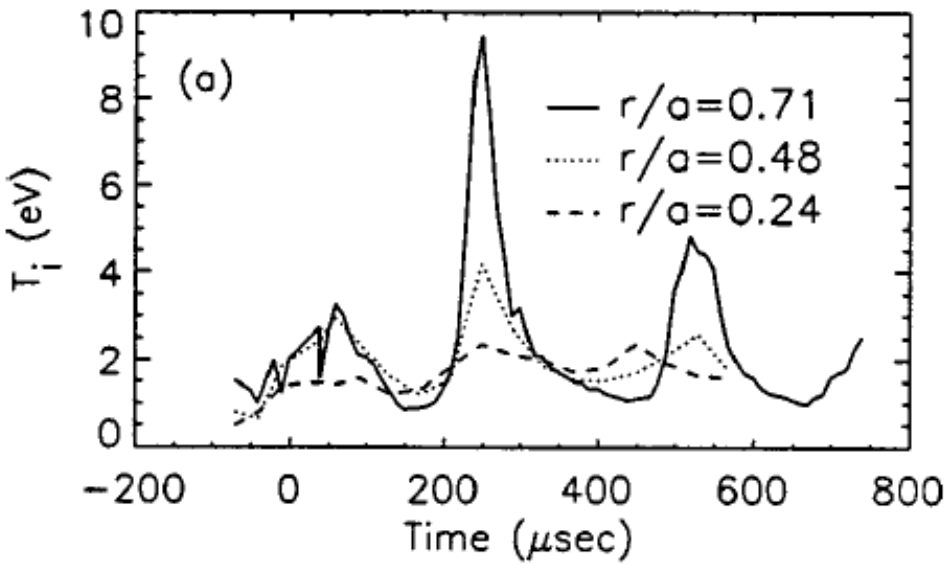

- Ion temperature at three different positions during the drift-Alfvén wave activity. Sanders *et al.*, Phys. Plasmas **5**, 716 (1998).

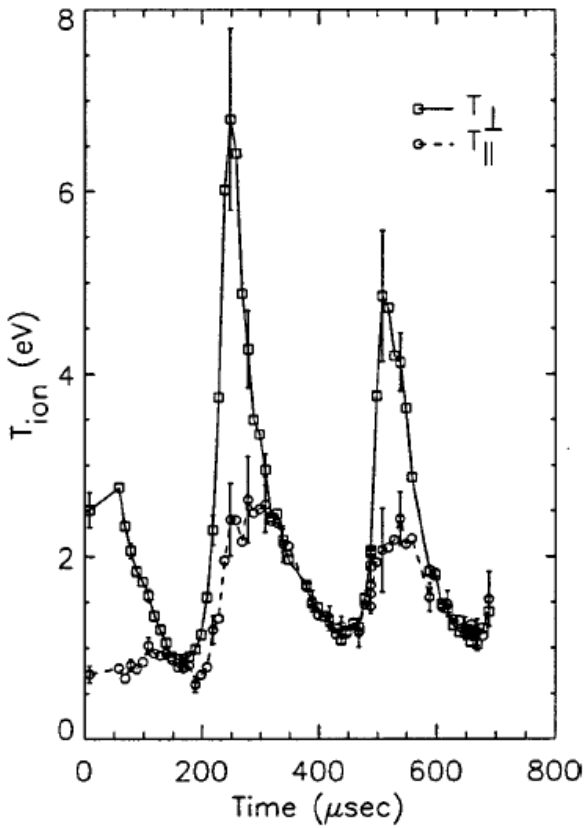

- Measured ion temperatures $T_\perp$ and $T_\parallel$. Wave period 230 μs. Sanders *et al.*, Phys. Plasmas **5**, 716 (1998).

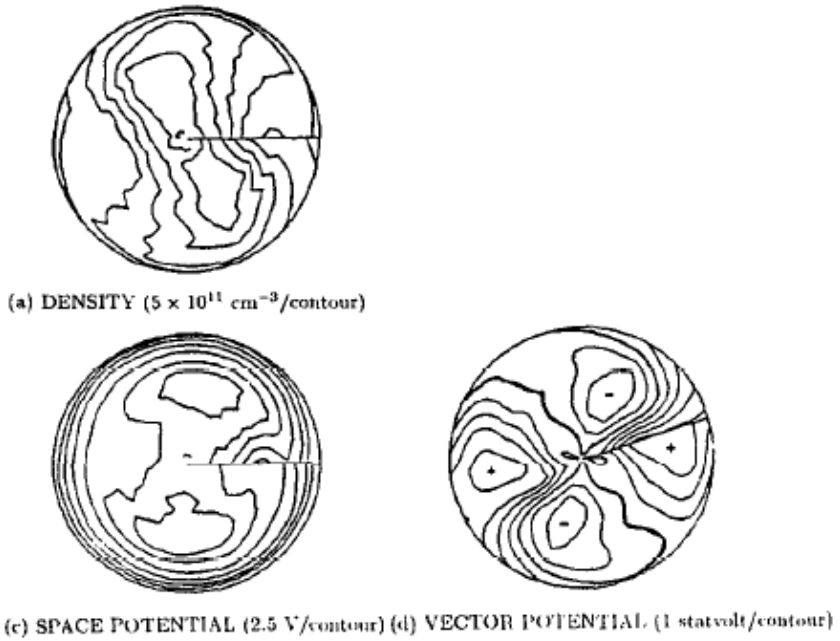

- Tokamak cross-section: drift-Alfvén wave structure ($m = 2$) during the heating.
- McChesney *et al.*, Phys. Fluids **B3**, 3363 (1991).

- Heating during coherent **(non-turbulent)** wave regime.

Outline

Collisional plasma; fluid description

- Geometry:

$$\vec{B}_0 = B_0 \vec{e}_z, \quad \nabla n_0 = -n_0' \vec{e}_x.$$

- Perturbations: $f(x)\exp[i(k_y y + k_z z - \omega t)]$, $|(df/dx)/f|, |(dn_{j0}/dx)/n_0| \ll k_y$
- The electron equations:

$$m_e n_e \left[\frac{\partial \vec{v}_e}{\partial t} + (\vec{v}_e \cdot \nabla)\vec{v}_e\right] = e n_e \nabla\phi - e n_e \vec{v}_e \times \vec{B} - \kappa T_e \nabla n_e$$
$$- m_e n_e \nu_{en}(\vec{v}_e - \vec{v}_n), \tag{1}$$

$$\frac{\partial n_{e1}}{\partial t} + \nabla_\perp (n_e \vec{v}_{\perp e}) + \nabla_z (n_{e0} \vec{v}_{ez1}) = 0. \tag{2}$$

- Neutrals:

$$\left[\frac{\partial \vec{v}_n}{\partial t} + (\vec{v}_n \cdot \nabla)\right] \vec{v}_n = -\nu_{ne}(\vec{v}_n - \vec{v}_e). \tag{3}$$

- The momentum conservation implies that $\nu_{ne} = m_e n_e \nu_{en}/(m_n n_n)$.
- Ions:

$$m_i n_i \left[\frac{\partial \vec{v}_i}{\partial t} + (\vec{v}_i \cdot \nabla)\vec{v}_i \right] = -e n_i \nabla \phi + e n_i \vec{v}_i \times \vec{B}. \tag{4}$$

$$\Omega_e \gg |\omega| \gg \Omega_i, \tag{5}$$

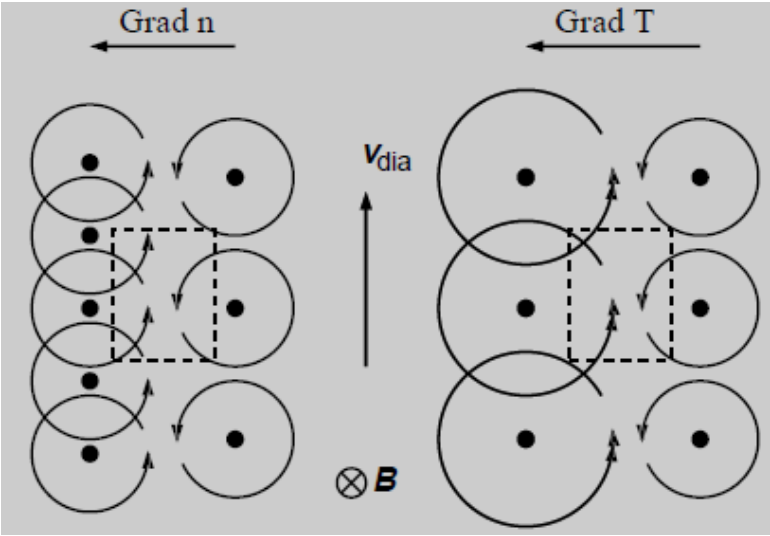

- from H. J. de Blank, Plasma Physics Lecture Notes
- free energy in the system

- Dispersion equation, the oblique, density gradient driven IA mode [Vranjes and Poedts, Phys. Plasmas **16**, 022101 (2009)]:

$$\frac{k^2 c_s^2}{\omega^2} = \frac{\omega_{*e} + iD_p + iD_z(\omega^2 + \nu_{ne}^2)/(\omega^2 - i\nu_{ne}\omega)}{\omega + iD_p + iD_z(\omega^2 + \nu_{ne}^2)/(\omega^2 - i\nu_{ne}\omega)}. \tag{6}$$

$$D_p = \nu_{en}\alpha k_y^2 \rho_e^2, \quad D_z = k_z^2 v_{Te}^2/\nu_{en}, \quad \rho_e = v_{Te}/\Omega_e.$$

$$\omega_{*e} = v_{*e} k_y, \quad \vec{v}_{*e} = -\frac{\kappa T_e}{eB_0}\vec{e}_z \times \frac{\nabla n_0}{n_0}, \quad \alpha = \omega/(\omega + i\nu_{ne}).$$

- $\alpha = 1 \Leftarrow$ static neutrals D_p - usually omitted without justification.
- ω_{*e} - diamagnetic frequency; introduces free energy.

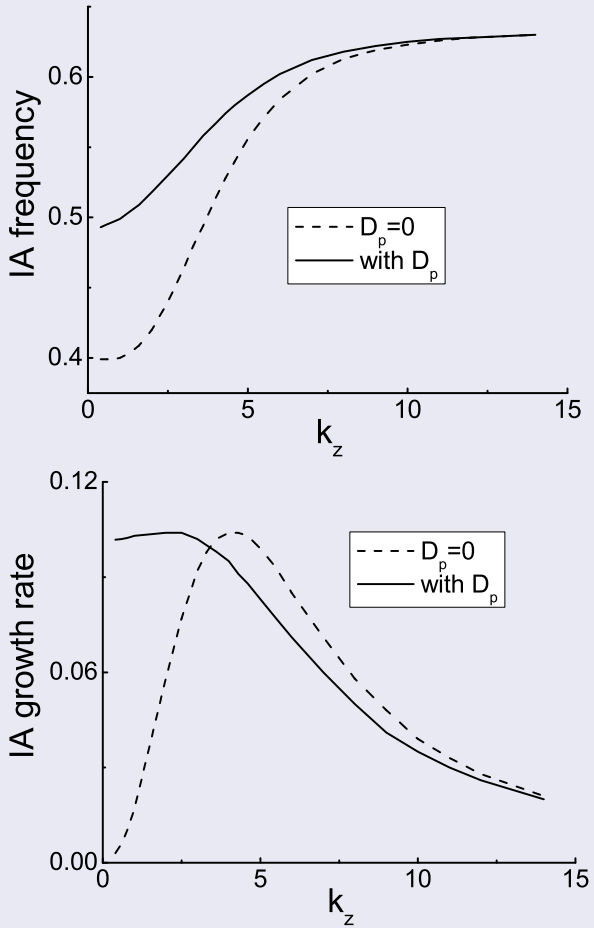

- Vranjes and Poedts, Phys. Plasmas **16**, 022101 (2009).
- Frequency (normalized to ω_{*e}), and the corresponding normalized growth-rate.
- Parameters: $m_i = 40 m_p$, $m_n = m_i$, $T_e = 5$ eV, $n_{n0} = 10^{21}$ m^{-3}, $n_{e0} = n_{i0} = 5 \cdot 10^{16}$ m^{-3}, $B_0 = 0.01$ T, $L_n = 0.1$ m, $k_y = 7 \cdot 10^2$ 1/m. For these parameters $\sigma_{en} = 8.7 \cdot 10^{-20}$ m^2.
- The perpendicular electron collisions drastically destabilize the mode. For small k_z, the growth rate about 70 times larger. Note that for $k_z = 0.3$ 1/m we have $D_p/D_z = 141$, while for $k_z = 14$ 1/m this ratio is only 0.06.

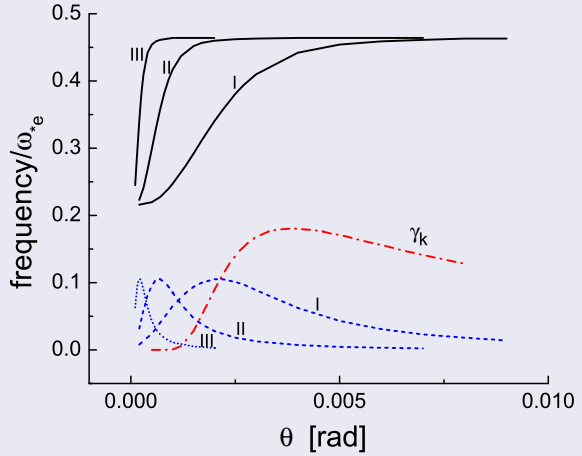

- Phys. Plasmas **17**, 022104 (2010).

- Angle dependence - angle of preference. Frequency (full lines) and the corresponding growth rates (dashed lines), both normalized to the electron diamagnetic drift frequency, for three values of neutral number density. The lines I, II, III correspond (respectively) to $n_{n0} = 10^{19}$, 10^{18}, 10^{17} m^{-3}.
- θ - arctan(k_z/k_y).
- The line γ_k is the kinetic growth-rate (for the same parameters as line II).

Kinetic instability

- Same geometry; magnetized (un-magnetized) electrons (ions); but no collisions.
- The perturbed number density for electrons (the same as for the drift wave):

$$\frac{n_{e1}}{n_0} = \frac{e\phi_1}{\kappa T_e}\left\{1 + i\left(\frac{\pi}{2}\right)^{1/2}\frac{\omega - \omega_{*e}}{k_z v_{Te}}\exp\left[-\omega^2/(2k_z^2 v_{Te}^2)\right]\right\}. \quad (7)$$

- The ion number density:

$$\frac{n_{i1}}{n_{i0}} = -\frac{e\phi_1}{m_i v_{Ti}^2}\left[1 - J_+\left(\frac{\omega_i}{k v_{Ti}}\right)\right]. \quad (8)$$

- Here, $J(\eta) = [\eta/(2\pi)^{1/2}]\int_c d\zeta \exp(-\zeta^2/2)/(\eta - \zeta)$ is the plasma dispersion function, and $\zeta = v/v_{Ti}$.

- Frequency and the growth rate from the quasi-neutrality:

$$\omega_k^2 = \frac{k^2 c_s^2}{2}\left[1 + (1 + 12\,T_i/T_e)^{1/2}\right]. \tag{9}$$

$$\gamma_k \simeq -\frac{(\pi/2)^{1/2}\omega_k^3}{2k^2 c_s^2}\times$$
$$\times\left\{\frac{\omega_k - \omega_{*e}}{k_z v_{Te}}\exp\left[-\omega_k^2/(2k_z^2 v_{Te}^2)\right] + \frac{T_e}{T_i}\frac{\omega_k}{k v_{Ti}}\exp\left[-\omega_k^2/(2k^2 v_{Ti}^2)\right]\right\}. \tag{10}$$

- The electron contribution in Eq. (10) yields a kinetic instability provided that $\omega_k < \omega_{*e}$.

Plasmas with macroscopic motion

Reminder: electron current driven instability of the IA wave.

- Electron flow along the magnetic field, or in arbitrary z-direction without the field. Kinetic instability:

$$\gamma = \left(\frac{\pi}{8}\right)^{1/2} k c_s \left[\left(\frac{m_e}{m_i}\right)^{1/2}\left(\frac{v_{e0}}{c_s} - 1\right) - \tau^{3/2}\exp\left(-\frac{\tau}{2}\right)\right]. \tag{11}$$

$$v_{e0} > c_s[1 + (m_i/m_e)^{1/2}\tau^{3/2}\exp(-\tau/2)], \quad \tau = T_e/T_i. \tag{12}$$

- Threshold high; for $\tau = 1$ it is $27c_s$.
- Two-fluid counterpart: electron-collision effect, even higher threshold! [Vranjes et al., Phys. Plasmas **13**, 122103 (2006)].

$$\gamma = -\frac{\nu_i}{2(1-\chi)}\left(1 - \frac{\nu_e}{\nu_i}\chi\right), \quad \chi = \frac{m_e}{m_i}\frac{k^2}{k_z^2}\left(\frac{k_z v_0}{\omega_r} - 1\right). \tag{13}$$

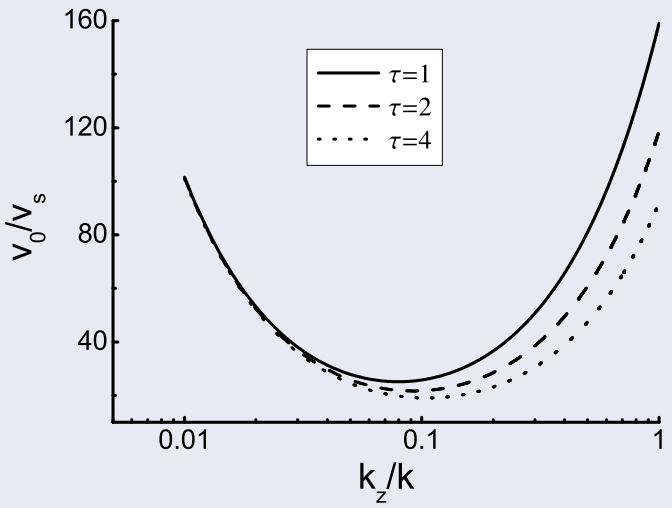

- Vranjes *et al.*, Phys. Plasmas **13**, 122103 (2006).
- Collisional instability threshold for electron-proton plasma in a H-gas.
- Angle dependent (with respect to the magnetic field) due to ion collisions.
- Un-magnetized ions, but this time due to collisions: $\nu_i > \Omega_i$.

Permeating plasmas: IA wave instability

- Two plasmas separately quasi-neutral

$$n_{fi0} = n_{fe0} = n_{f0}, \quad n_{si0} = n_{se0} = n_{s0}. \tag{14}$$

- Instability threshold; below the sound speed of the static plasma.
- Current-less instability.
- The ion Doppler shift appears to play the main role.
- Examples:
  - colliding astrophysical clouds,
  - stellar/solar winds propagation through interplanetary/interstellar space,
  - in the solar atmosphere.

Solar wind

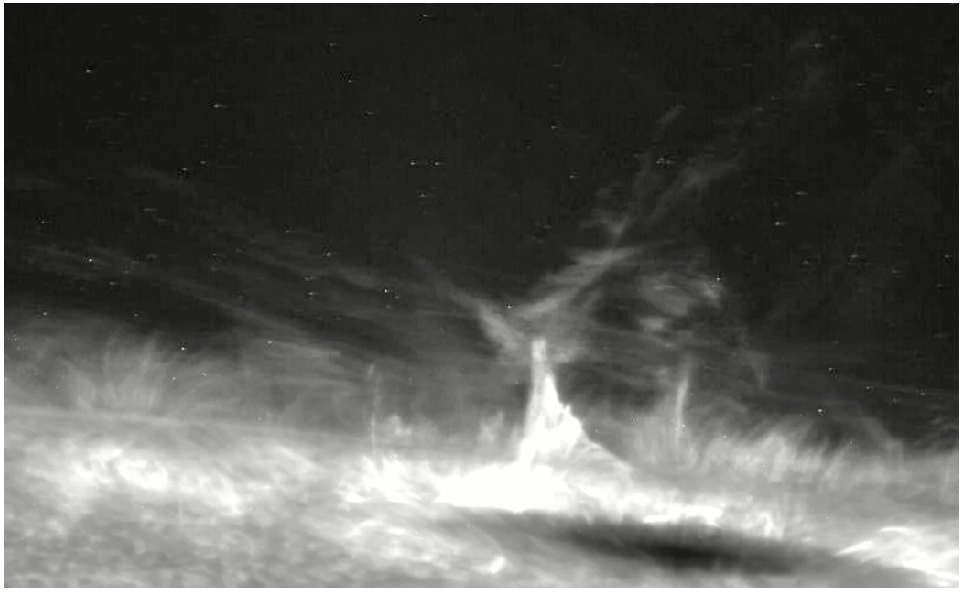

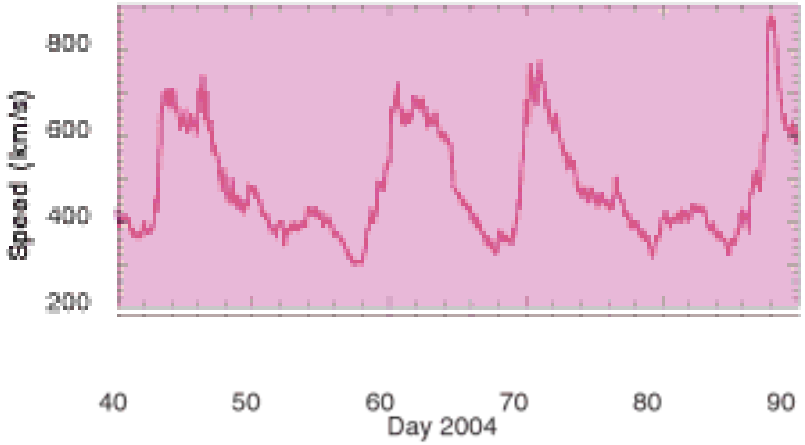

- *Encyclopedia of the solar system*, eds. L. A. McFadden *et al.*.
- 1-hour average solar wind at 1 AU.

- The IA wave dispersion equation [Vranjes *et al.*, Phys. Plasmas **16**, 074501 (2009)]

$$\Delta(k,\omega) \equiv 1 + \frac{1}{k^2\lambda_d^2} - \frac{\omega_{psi}^2}{\omega^2} - \frac{3k^2 v_{Tsi}^2 \omega_{psi}^2}{\omega^4}$$

$$+i\left(\frac{\pi}{2}\right)^{1/2}\left[\underbrace{\frac{\omega\omega_{pse}^2}{k^3 v_{Tse}^3}}_{c} + (\omega - kv_{f0})\left(\underbrace{\frac{\omega_{pfe}^2}{k^3 v_{Tfe}^3}}_{a} + \underbrace{\frac{\omega_{pfi}^2}{k^3 v_{Tfi}^3}}_{b}\right) + \frac{\omega\omega_{psi}^2}{k^3 v_{Tsi}^3}\exp\left(-\frac{\omega^2}{2k^2 v_{Tsi}^2}\right)\right] = 0. \qquad (15)$$

$$1/\lambda_d^2 = 1/\lambda_{dse}^2 + 1/\lambda_{dfe}^2 + 1/\lambda_{dfi}^2, \quad \lambda_{dse} = v_{Tse}/\omega_{pse}, \quad \text{etc.}$$

- The inertia of the mode provided by the static ions.
- $a/b \ll 1 \Leftarrow$ electron flow contribution negligible.

Laboratory plasma

- General case; numerical solution

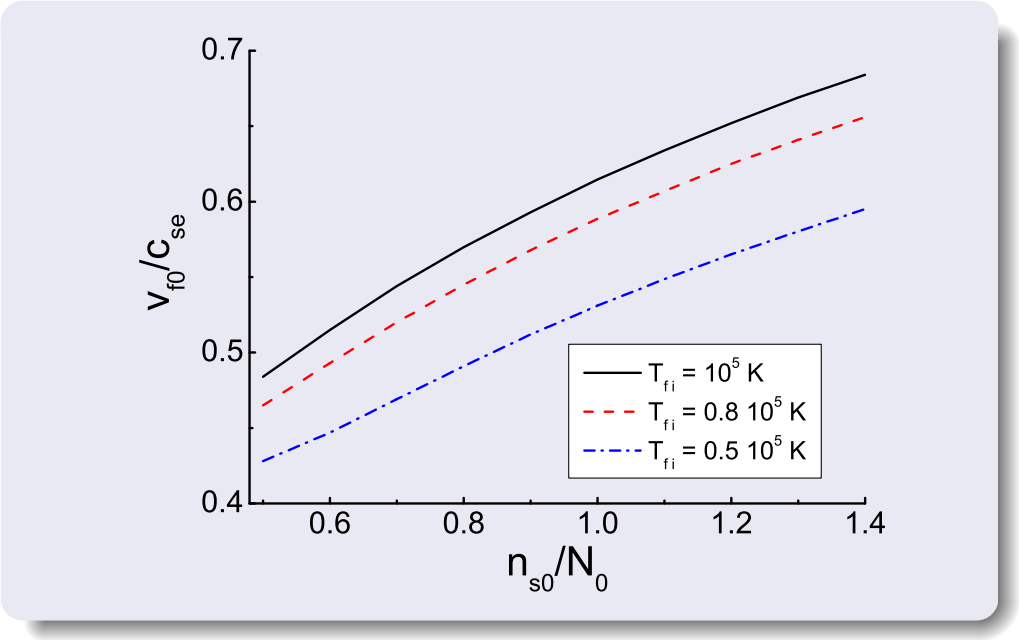

- Vranjes *et al.*, Phys. Plasmas **16**, 074501 (2009).
- The critical (threshold) values of the flowing plasma velocity for the ion-acoustic wave instability in terms of the number density of the static (target) plasma; $c_{se}^2 = \kappa T_{se}/m_i$.

Solar plasma

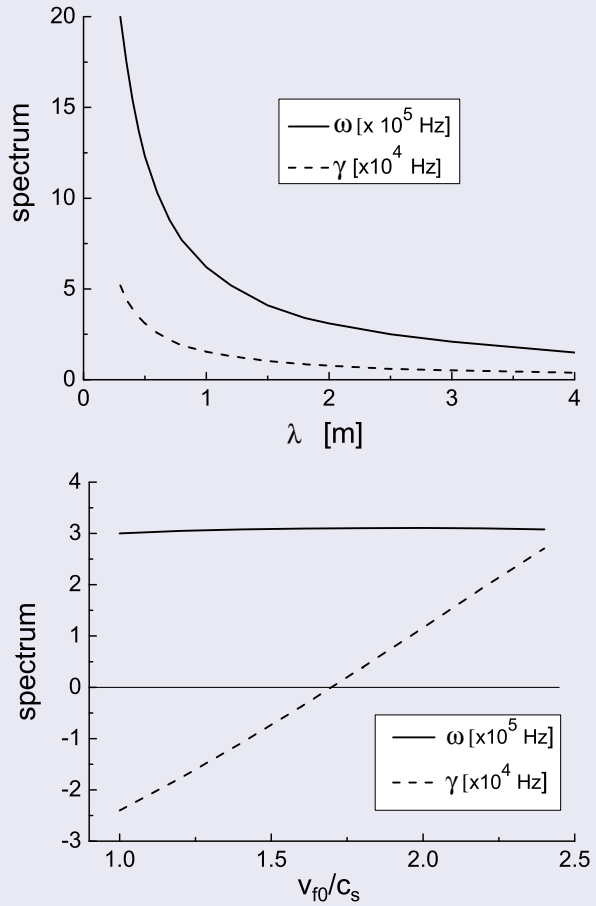

- **Upper.** Full line: IA wave frequency. Dashed line: the corresponding growth rate.
- **Lower.** Spectrum dependence on the speed of the flowing plasma.

Outline

In cylindric geometry

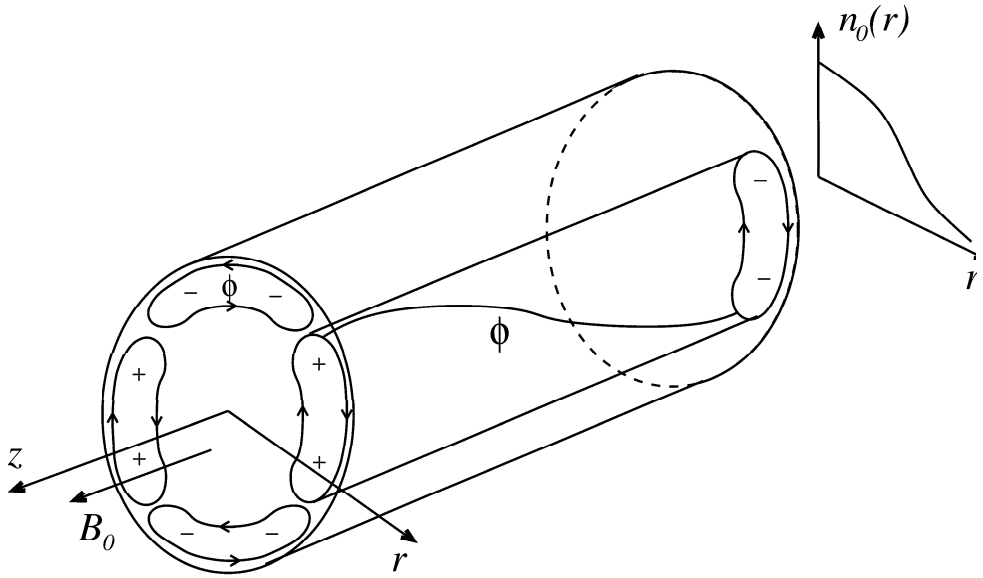

- A drift wave in cylindric geometry with poloidal wave number $m = 2$. From Vranjes and Poedts, MNRAS **398**, 918 (2009).

Cross section in cylindric geometry

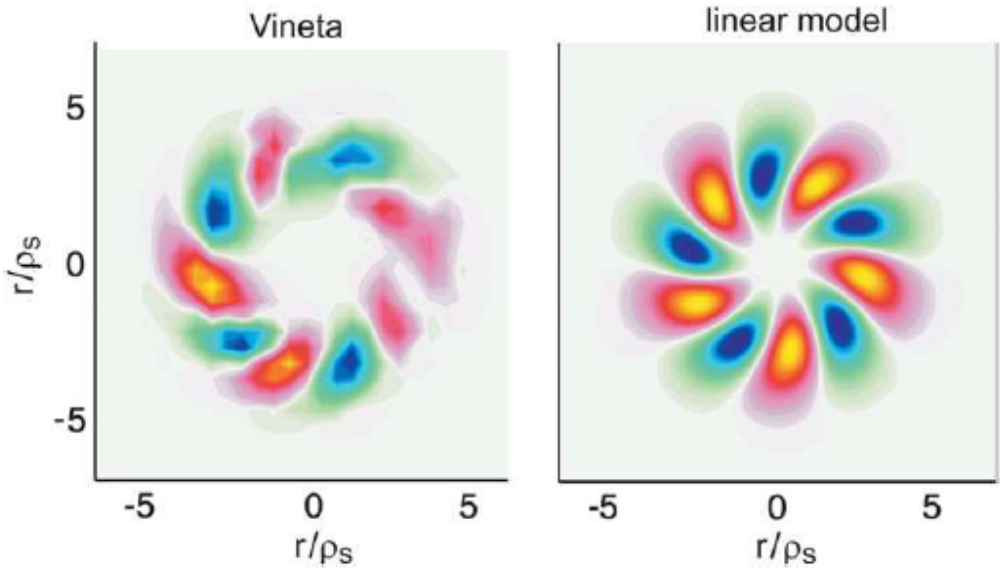

- The cross-section of an experimentally observed drift mode with the poloidal number m = 5 in a cylindric VINETA device (left) and the corresponding analytical solutions (right). From Grulke O., et al., Plasma Phys. Control. Fusion 49, B247 (2007).

Toroidal geometry

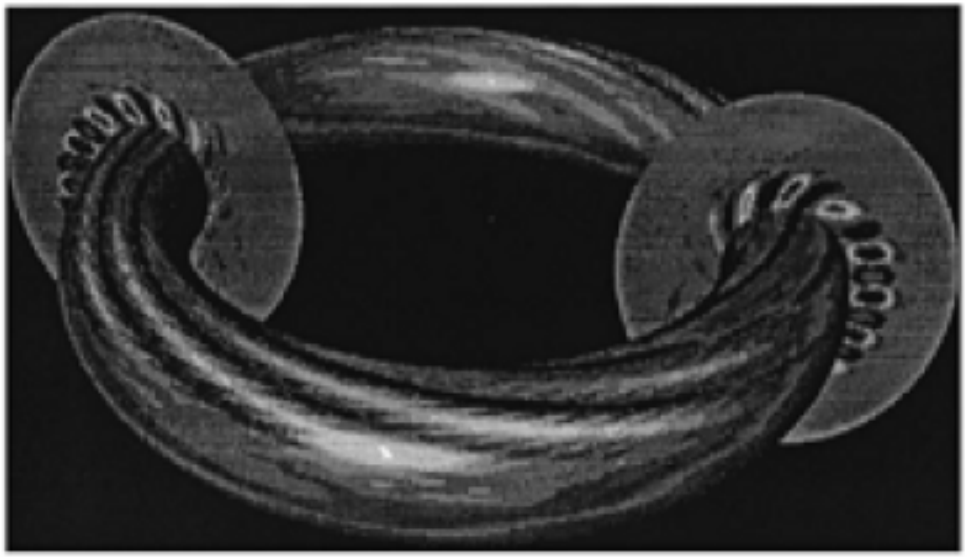

- Typical geometry of the drift wave in a torus; from Horton, Rev. Mod. Phys. **71**, 735 (1999).

- Experimentally investigated more than any other plasma mode.
- Naturally coupled to the ion acoustic wave and Alfvén wave
  - $\Rightarrow$ drift-Alfvén mode.

Experiments in Japan

Experimental Apparatus (HYPER-I)

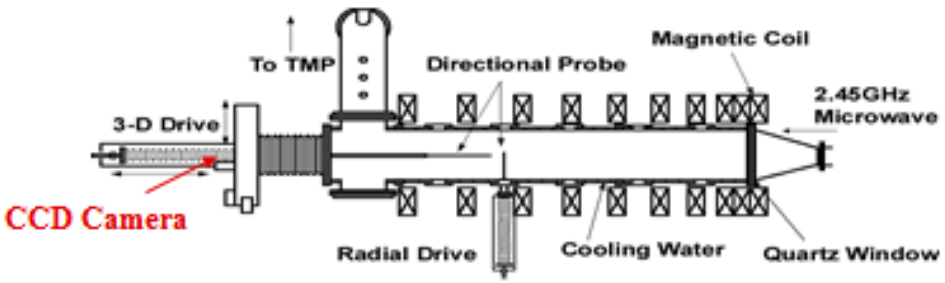

Parameters

Power	4-15	kW
Frequency	2.45	GHz
Magnetic Field	1	kG
Gas (He)	6×10^{-4}	Torr
El. Temp.	20	eV
El Density	10^{12}	cm^{-3}

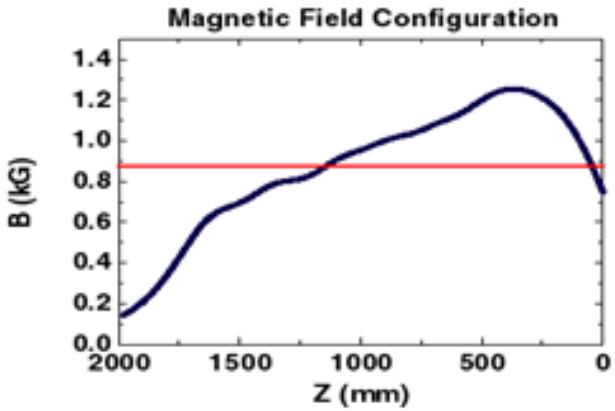

The experiments have been performed with the High Density Plasma Experiment (HYPER-I) device at National Institute for Fusion Science. The plasmas are produced by electron cyclotron resonance heating. The magnetic field configuration is a so-called magnetic beach structure. The plasma discharge time is ~60s and a helium gas is used with the operation pressures 6 ~ 8 x 10^{-4} Torr.

Experiments in Japan

Group of Kono & Tanaka

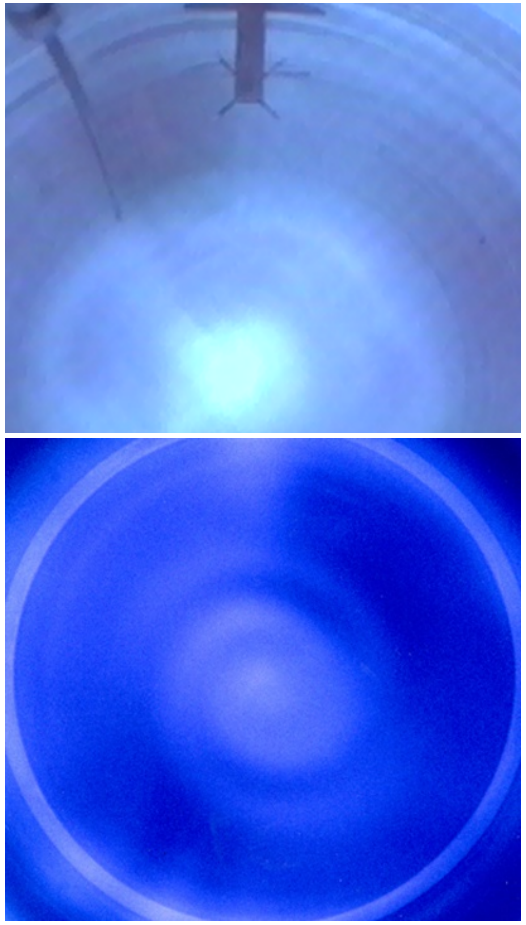

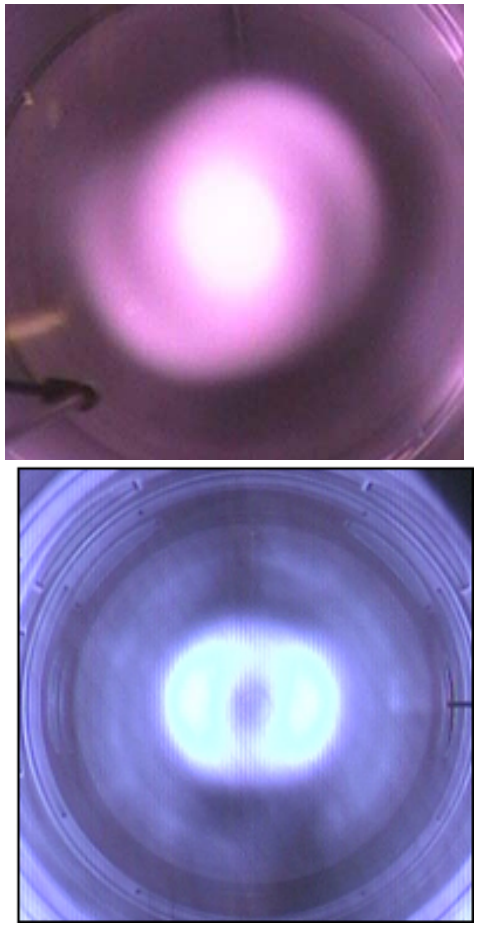

Experiments in Japan

Group of Kono & Tanaka

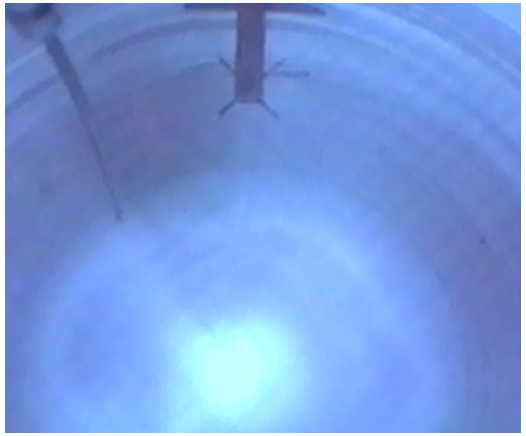

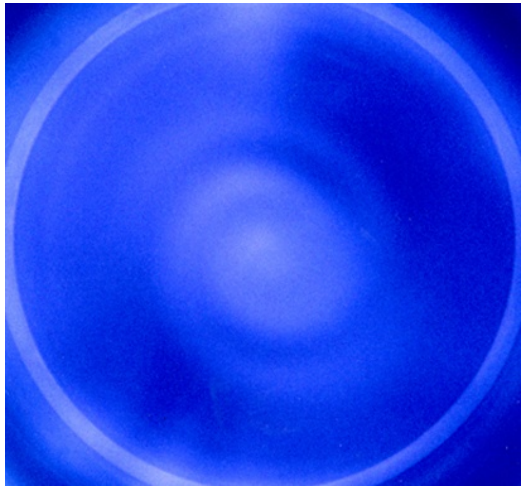

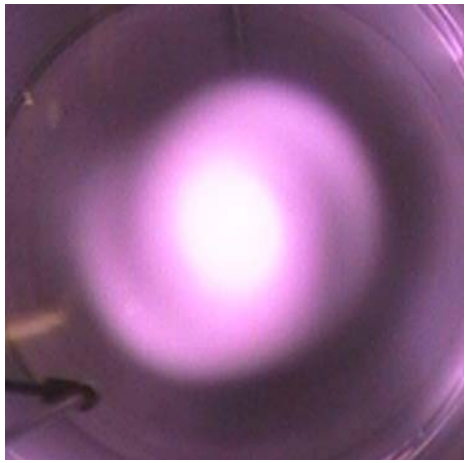

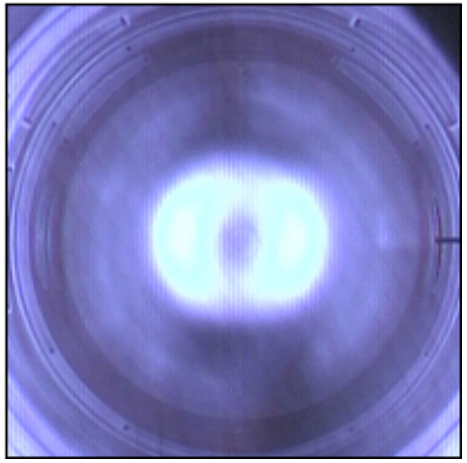

Experiments in Japan

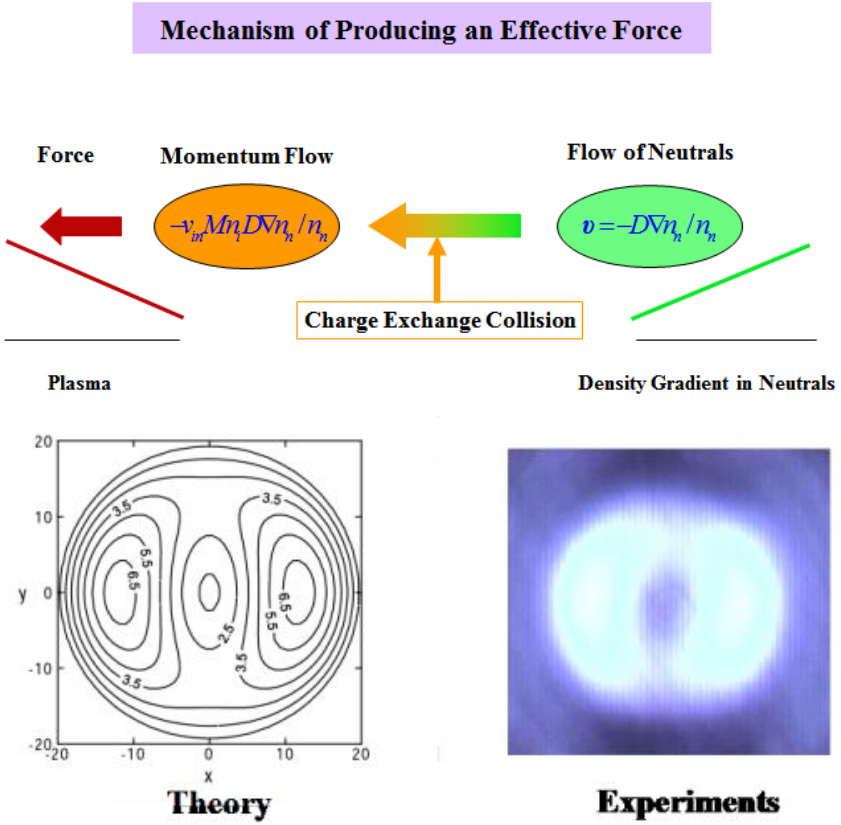

- Vranjes *et al.*, Phys. Rev. Lett. **89**, 265002 (2002).

Solar drift wave lab

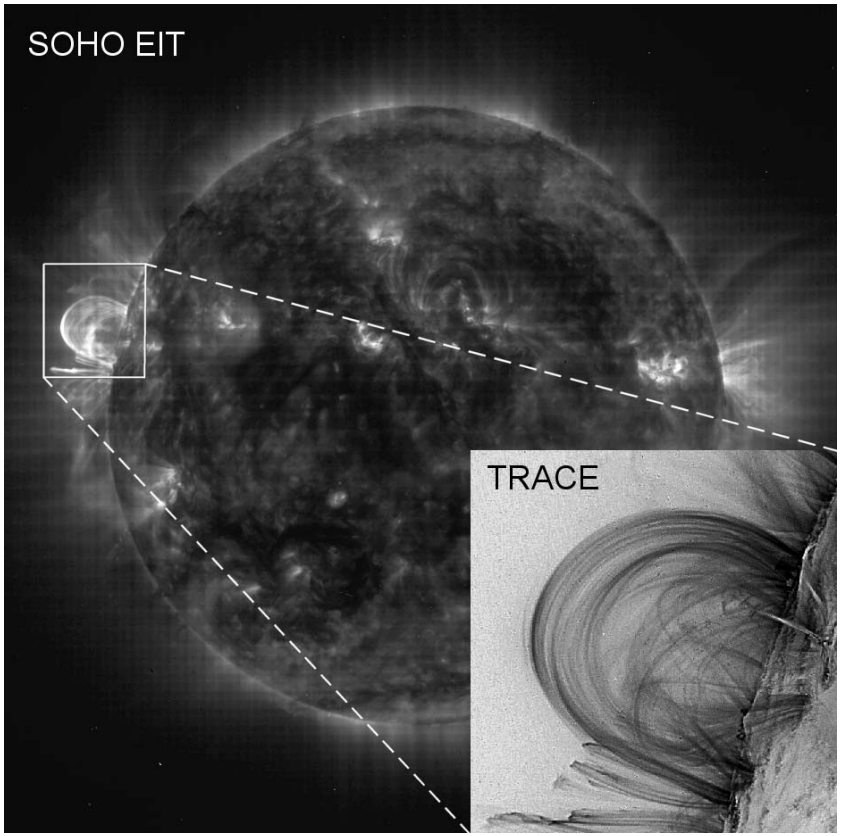

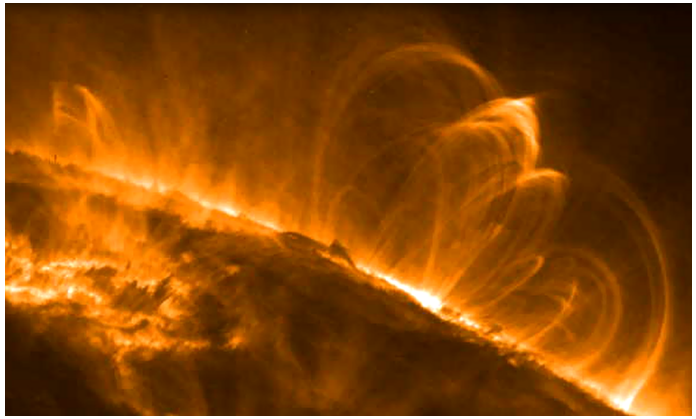

Oblique drift wave properties

Universally unstable:

- Collisional and collision-less instability within fluid theory
  - J. Vranjes and S. Poedts, Astron. Astrophys. **458**, 635 (2006),
  - H. Saleem, J. Vranjes, and S. Poedts, Astron. Astrophys. **471**, 289 (2007),
  - J. Vranjes and S. Poedts, MNRAS **400**, 2147 (2009).
- Collision-less instability within kinetic theory
  - J. Vranjes and S. Poedts, MNRAS **398**, 918 (2009),
  - J. Vranjes and S. Poedts, Astrophys. J. **719**, 1335 (2010).
- Current driven instability.
- Shear-flow driven instability.
- Trapped particle instability.
- Nonlinear instability.

Minimum conditions and equations

- Geometry:

$$\vec{B}_0 = B_0 \vec{e}_z, \quad \nabla n_0 = -n_0' \vec{e}_x.$$

- Perturbations: $f(x)\exp[i(k_y y + k_z z - \omega t)]$.
- Boltzmannian electrons (implying that $\omega/k_z \ll v_{Te}$, $v_{ze} \ll v_{Te}$, and on condition $e\phi_1/(\kappa T_e) \ll 1$):

$$\frac{n_{e1}}{n_0} = \frac{e\phi_1}{\kappa T_e}. \tag{16}$$

- Cold ions ($v_{Ti} \ll \omega/k_z$) motion strictly perpendicular (to $\vec{B}_0 = B_0 \vec{e}_z$) implying that $\omega/k_z \gg c_s$; low frequency perturbations $\omega \ll \Omega_i$

$$m_i n_i \left(\frac{\partial \vec{v}}{\partial t} + \vec{v} \cdot \nabla \vec{v} \right)_i = n_i e \left(-\nabla \phi + \vec{v}_i \times B_0 \right).$$

$$\vec{v}_{\perp i1} = \frac{1}{B_0} \left(\vec{e}_z \times \nabla \phi_1 \right) - \frac{1}{\Omega_i B_0} \frac{\partial}{\partial t} \nabla \phi_1, \quad v_{\parallel i} = \frac{k_z}{\omega} \frac{e\phi_1}{m_i}.$$

- The ion continuity

$$\frac{\partial n_i}{\partial t} + \nabla \cdot n_i \vec{v}_i = 0.$$

- Dispersion equation in local approximation

$$\omega^2 \left(1 + k_y^2 \rho_s^2 \right) - \omega \omega_{*e} - k_z^2 c_s^2 = 0, \quad \omega_{*e} = k_y v_{*e}, \quad \vec{v}_{*e} = -\frac{\kappa T_e}{e B_0} \frac{1}{n_0} \frac{dn_0}{dx} \vec{e}_y,$$

$$\rho_s = c_s / \Omega_i, \quad c_s^2 = \kappa T_e / m_i.$$

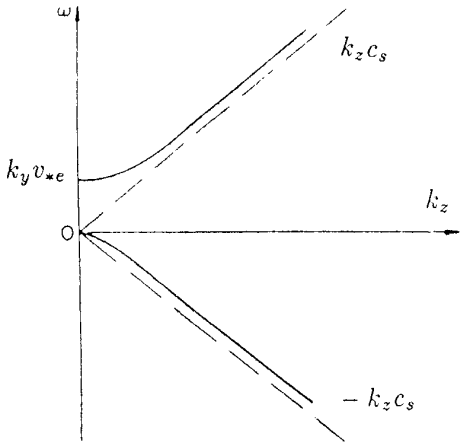

- Coupled drift and ion acoustic waves.

- Electron collisions

$$\frac{n_{e1}}{n_0} = \frac{e\phi_1}{\kappa T_e}\left[1 - i\frac{m_e \nu_{ei}}{k_z^2 \kappa T_e}(\omega_{*e} - \omega)\right]. \tag{17}$$

- Growth rate:

$$\gamma = \frac{\nu_e \omega_r^2 \rho_s^2 k_y^2}{k_z^2 v_{Te}^2}. \tag{18}$$

Solar atmosphere: source 1 - collisional instability

In Cartesian geometry, for perturbations $\sim\exp(-\mathrm{i}\omega t+\mathrm{i}k_y y+\mathrm{i}k_z z)$,

$$\omega^3-\omega^2\left[\omega_{*\mathrm{e}}+\omega_{*\mathrm{i}}-\mathrm{i}\left(\delta+\frac{\nu_\mathrm{i}}{1+k_y^2\rho_\mathrm{i}^2}\right)\right]$$

$$+\omega\left\{\omega_{*\mathrm{e}}\omega_{*\mathrm{i}}-\frac{k_z^2c_a^2}{1+k_y^2\rho_\mathrm{i}^2}-k_y^2k_z^2c_a^2\left(\rho_s^2+\rho_\mathrm{i}^2\right)-\frac{\nu_\mathrm{i}\delta}{1+k_y^2\rho_\mathrm{i}^2}\right.$$

$$\left.-\mathrm{i}\left[\omega_{*\mathrm{i}}\delta+\frac{\nu_\mathrm{i}(\omega_{*\mathrm{e}}+\omega_{*\mathrm{i}})}{1+k_y^2\rho_\mathrm{i}^2}\right]+\frac{\omega_{*\mathrm{e}}k_z^2c_a^2}{1+k_y^2\rho_\mathrm{i}^2}+\frac{\omega_{*\mathrm{i}}\nu_\mathrm{i}\delta}{1+k_y^2\rho_\mathrm{i}^2}\right\}$$

$$+\mathrm{i}\frac{\nu_\mathrm{i}}{1+k_y^2\rho_\mathrm{i}^2}\left[\omega_{*\mathrm{e}}\omega_{*\mathrm{i}}-k_z^2c_a^2k_y^2\left(\rho_s^2+\rho_\mathrm{i}^2\right)\right]=0.$$

$\omega_{*\mathrm{e}}=k_yv_{\mathrm{e}0}$, $v_{\mathrm{e}0}=-\kappa T_\mathrm{e}\kappa_0/(eB_0)$, $\kappa_0=n_0'/n_0$, $\omega_{*\mathrm{i}}=k_yv_{\mathrm{i}0}$, $v_{\mathrm{i}0}=\kappa T_\mathrm{i}\kappa_0/(eB_0)$, $\delta=m_\mathrm{e}\nu_\mathrm{e}k_y^2/(\mu_0n_0e^2)$.

- Vranjes and Poedts, Astron. Astrophys. **458**, 635 (2006).

- Interaction with Alfvén waves.

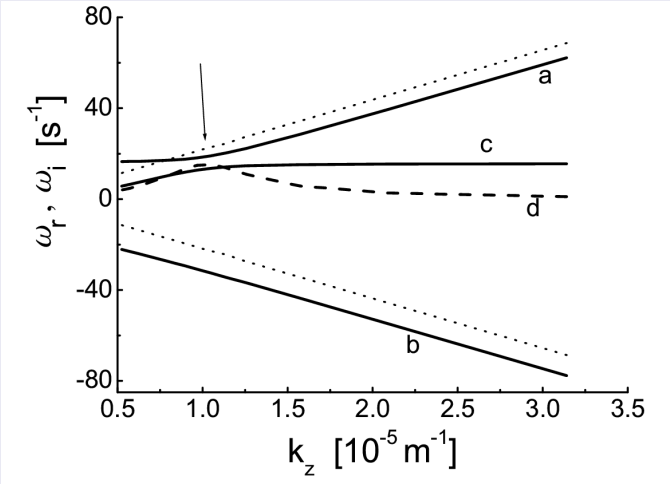

- growing drift wave mode
  $\rightarrow$ locally increased plasma-β
  $\rightarrow$ electromagnetic effects
  $\rightarrow$ excitation of (growing) AW.
  - exchange of identities, Vranjes and Poedts, AA **458**, 635 (2006).
  $\rightarrow$ reconnection (consequence of heating)

Source 2: shear flow instability in solar spicules

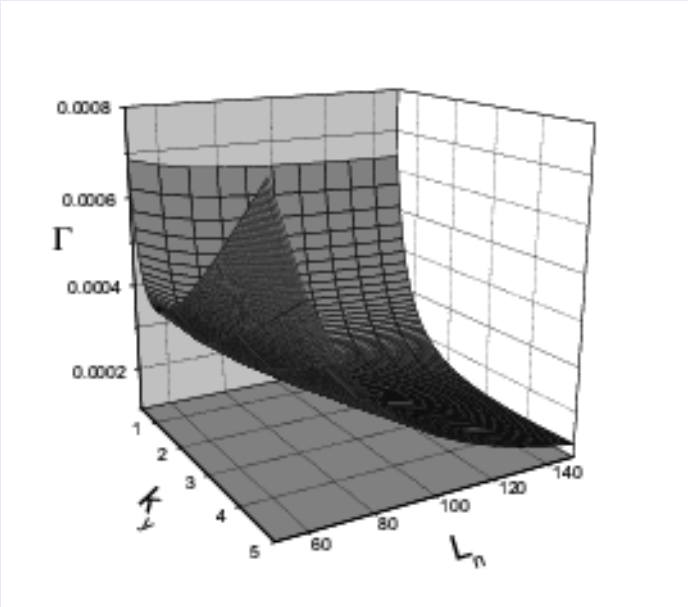

- Saleem, Vranjes and Poedts, Astron. Astrophys. **471**, 289 (2007).

- The minimal value of the normalized shear $\Gamma = dv_{z0}(x)/(\Omega_i dx)$ in terms of k_y and L_n. Instability for the values above the surface.

Source 3: kinetic drift wave instability

$$\omega_r = -\frac{\omega_{*i}\Lambda_0(b_i)}{1-\Lambda_0(b_i)+T_i/T_e+k_y^2\lambda_{di}^2},$$

$$\gamma \simeq -\left(\frac{\pi}{2}\right)^{1/2}\frac{\omega_r^2}{|\omega_{*i}|\Lambda_0(b_i)}\left[\frac{T_i}{T_e}\frac{\omega_r-\omega_{*\mathbf{e}}}{|k_z|v_{Te}}\exp[-\omega_r^2/(k_z^2v_{Te}^2)]\right.$$
$$\left.+\frac{\omega_r-\omega_{*i}}{|k_z|v_{Ti}}\exp[-\omega_r^2/(k_z^2v_{Ti}^2)]\right].$$

$$\Lambda_0(b_i)=I_0(b_i)\exp(-b_i),\ \ b_i=k_y^2\rho_i^2,\ \ \lambda_{di}=v_{Ti}/\omega_{pi},\ \ \omega_{*e}=-k_y\frac{v_{Te}^2}{\Omega_e}\frac{n'_{e0}}{n_{e0}}\quad \omega_{*i}=k_y\frac{v_{Ti}^2}{\Omega_i}\frac{n'_{i0}}{n_{i0}}.$$

- the presence of the energy source seen already in the real part of the frequency $\omega_r \propto \nabla_\perp n_0$.

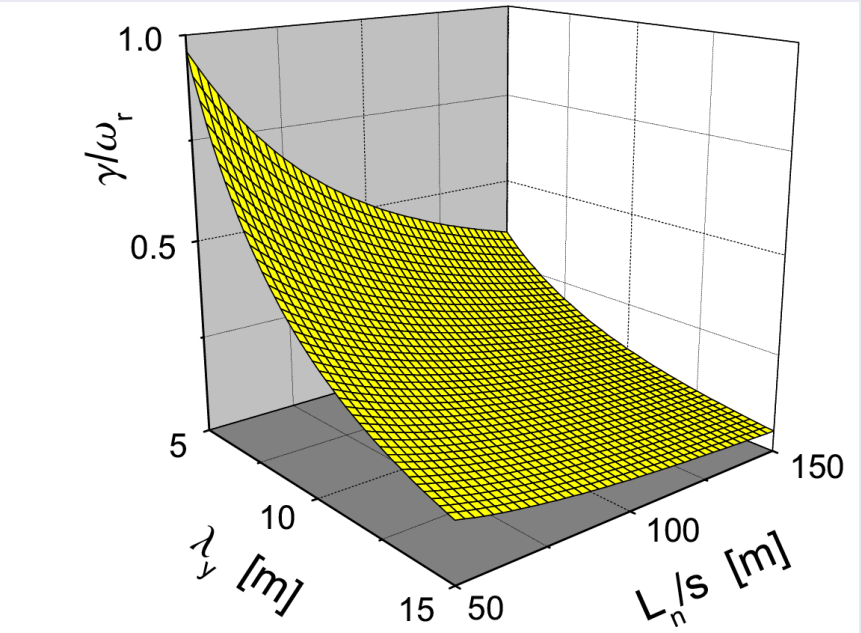

- Vranjes and Poedts, MNRAS **398**, 918 (2009).

- Kinetic growth rate normalized to the wave frequency ω_r in terms of the perpendicular wavelength λ_y and the density scale-length L_n, for $\lambda_z = s \cdot 2 \cdot 10^4$ m, $s \in (0.1, 10^3)$.
- Short perpendicular scale length; comparable to gyro-radius.

Polarization drift effects within the two-fluid description

$$v_{i\perp} = \frac{1}{B_0}\vec{e}_z \times \nabla_\perp \phi + \frac{v_{Ti}^2}{\Omega_i}\vec{e}_z \times \frac{\nabla_\perp n_i}{n_i} + \vec{e}_z \times \frac{\nabla_\perp \cdot \pi_i}{m_i n_i \Omega_i}$$
$$+\frac{1}{\Omega_i}\frac{d}{dt}\vec{e}_z \times \vec{v}_{i\perp}, \quad \frac{d}{dt} \equiv \frac{\partial}{\partial t} + \vec{v}\cdot\nabla. \tag{19}$$

- Guiding center approximation violated:

$$\vec{v}_{pi} = -\vec{e}_y \frac{\omega_r k_y \phi_1(t)}{B_0 \Omega_i}\left[\left(1 - \frac{k_z}{\omega_r}\frac{dz}{dt}\right)\cos\varphi - \frac{\gamma}{\omega_r}\sin\varphi\right] \times$$
$$\times 1/\left(1 - \frac{k_y^2 \phi_1(t)}{B_0 \Omega_i}\cos\varphi\right), \quad \varphi = k_y y(t) + k_z z(t) - \omega_r t. \tag{20}$$

Stochastic heating: individual particle dynamics

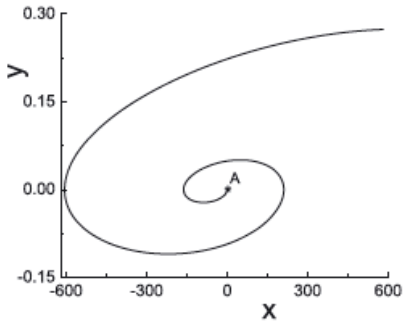

Figure 2. Normalized particle positions in the x–y plane, after it starts from the point A with $(x, y, z) = (0, 0, 0)$, for a growing electric field potential $\phi_1(t) = \hat{\phi}\ \exp(\gamma t/\Omega_i)$ and $\hat{\phi} = 0.86\,\mathrm{V}$.

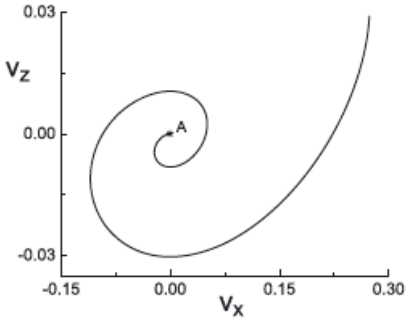

Figure 3. Normalized velocities v_x, v_z for the same parameters as in Fig. 2.

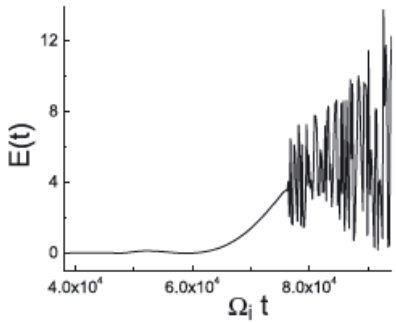

Figure 4. Change in time of the normalized kinetic energy of a particle with a unit mass $E = (v_x^2 + v_y^2 + v_z^2)/2$.

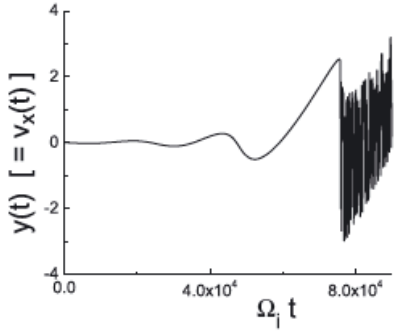

Figure 5. Normalized displacement in the direction of the polarization drift $y(t)$, and the normalized perpendicular velocity component $y(t) = v_x(t)$.

- Vranjes and Poedts, MNRAS **408**, 1835 (2010).

Numbers

- Frequency limits: $\omega < \Omega_i$, $\omega < \omega_{*e} = v_{*e} k_\perp$; $v_{*e} = -\frac{\kappa T_e}{eB_0} \vec{e}_z \times \frac{\nabla n_0}{n_0} \sim 1/L_n$.
- $L_n = 100$ m $\Rightarrow \omega \simeq 250$ Hz; $\gamma/\omega = 0.26$; growth time $\tau_g = 0.06$ s; energy release rate $\Gamma \simeq 0.7$ J/m^{3}s.
- $L_n = 100$ km $\Rightarrow \omega \simeq 0.25$ Hz; $\gamma/\omega = 0.28$; growth time $\tau_g = 60$ s; energy release rate $\Gamma \simeq 6 \cdot 10^{-4}$ J/m^{3}s.
- Maximum achieved particle speed:

$$v_{max} = \left(k_y^2 \rho_i^2 \frac{e\phi}{\kappa T_i} + 1.9 \right) \frac{\Omega_i}{k_y} \quad \Rightarrow \quad T_{eff}.$$

Properties

- Crucial electrostatic nature of the wave in the given process of heating.
  - yet, coupling to the Alfvén wave included!
- Highly anisotropic, takes place mainly in the direction normal to the magnetic field B_0 (both the $x-$ and y-direction velocities are stochastic).
- Electric fields of (tens) kV/m.
- Energy release rate in the range of nano-flares.
- Predominantly acts on ions

- Stronger heating of heavy ions

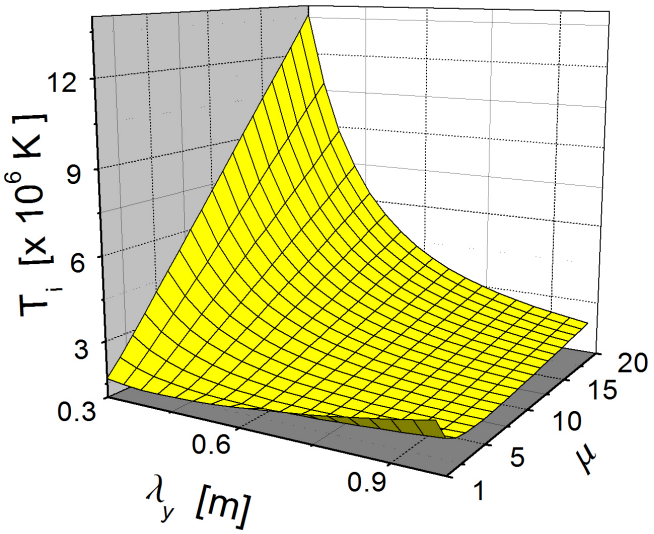

- The stochastically increased ion temperature $T_{eff} = m_i v_{max}^2/(3\kappa)$ (in millions K) in terms of the perpendicular wave-length λ_y and the ion mass.

- The areas with stronger background magnetic fields are subject to stronger stochastic heating.

- Particle acceleration in the parallel direction.

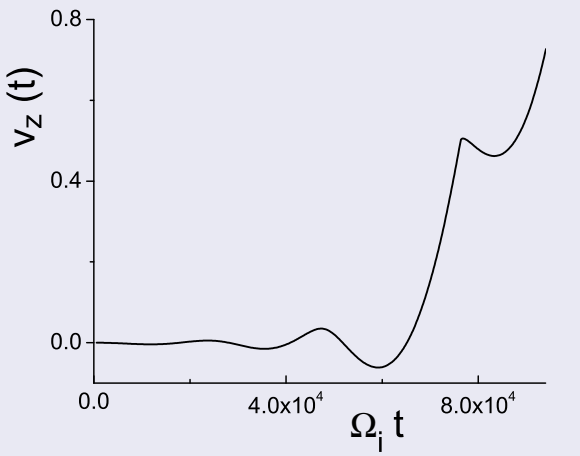

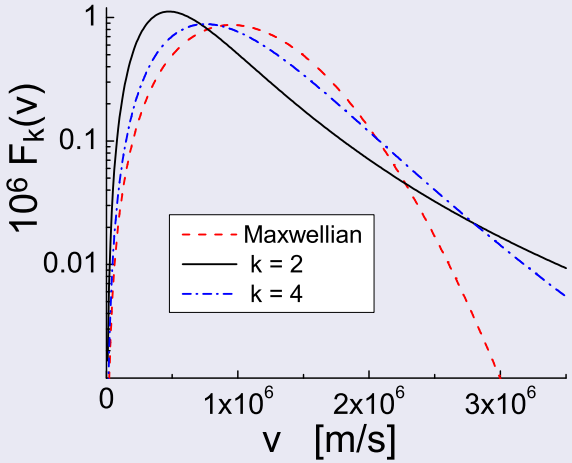

- Normalized perturbed velocity in the direction parallel to the magnetic field.

- Because the mean free path $\sim v^4 \Rightarrow$ kappa distribution.

Outline

Properties of the transverse drift wave

$$\vec{B}_0 = B_0\vec{e}_z, \quad \nabla n_0 = (dn_0/dx)\vec{e}_x, \quad \vec{k} = k\vec{e}_y, \quad \vec{k}\cdot\vec{B}_0 = 0,$$

$$\vec{E}_1 \parallel \vec{B}_0, \quad \vec{B}_1 \parallel \vec{B}_0, \quad \vec{B}_1 = (kE_1/\omega)\vec{e}_x.$$

In the limit $k_y\rho_i < 1$ [Krall & Rosenbluth, Phys. Fluids **6**, 254 (1963)]

$$\omega_r = -\frac{k_y\kappa T_e}{en_0B_0}\frac{dn_0}{dx}\frac{1}{1+k_y^2c^2/\omega_{pe}^2}, \quad \epsilon_{n,b} = 1/L_{n,b},$$

$$\frac{\gamma}{\omega_r} = \pi\frac{m_e}{m_i}\frac{\epsilon_n}{\epsilon_b}\left(1+\frac{k_y^2c^2}{\omega_{pe}^2}\right)^{-2}\left(1+\frac{k_y^2c^2}{\omega_{pe}^2}+\frac{T_e}{T_i}\right)$$

$$\times\exp\left\{-\frac{\epsilon_n}{\epsilon_b}\frac{T_e}{T_i}\frac{1}{1+k_y^2c^2/\omega_{pe}^2}\right\}, \quad \Leftarrow \text{no threshold!}$$

Motivation: transport

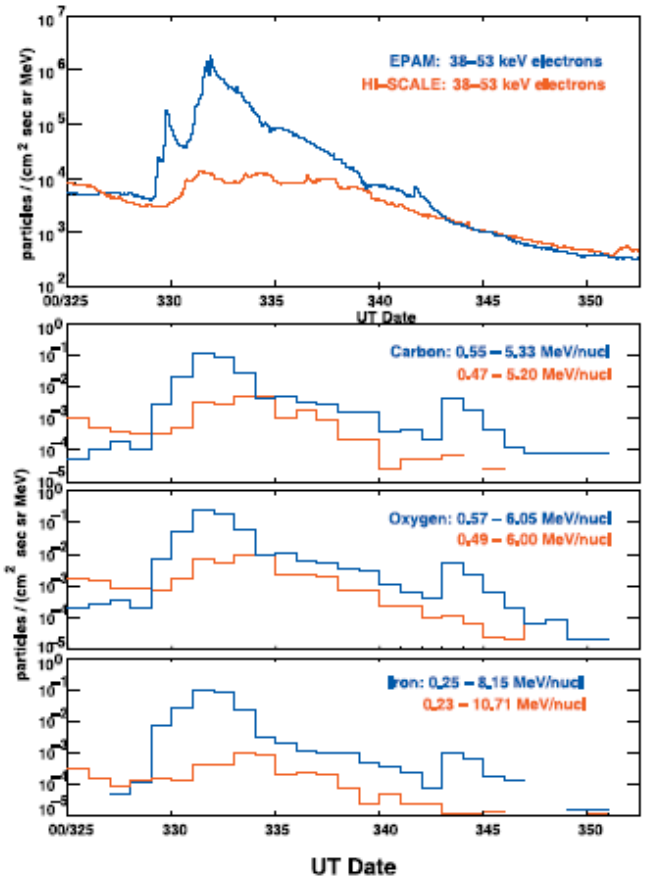

Figure 4. Comparisons of intensity-time traces of electrons and C, O, Fe ions measured during a small solar event at Ulysses (red) at ~80°S heliolatitude and in the ecliptic on ACE (blue).

- Particle transport to high latitudes.
- C. G. Maclennan *et al.*, Geophys. Res. Lett. **30**, 198033 (2003).
- ACE = Advanced Composition Explorer

- D. Lario *et al.*, Adv. Space Res. **32**, 579 (2003).
- Delays longer than for a spiral magnetic connection.
- Rise-time at ACE much faster ⇒ more diffusive transport at high lat.

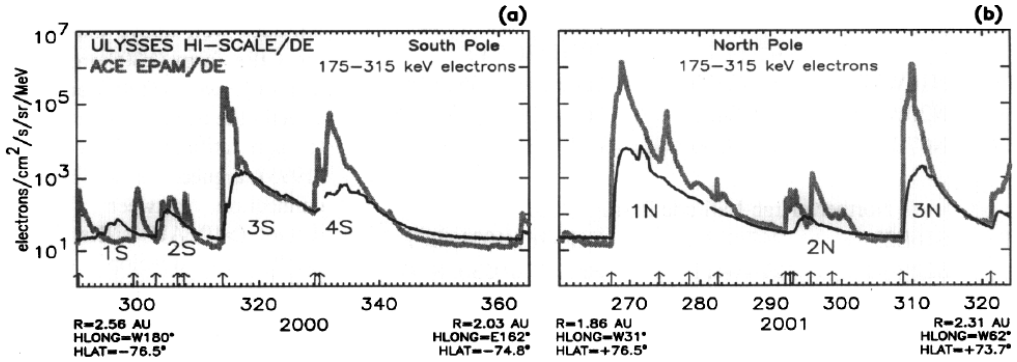

Fig. 2. Hourly averages of the 175-315 keV electron intensities as measured by Ulysses/HI-SCALE (black traces) and ACE/EPAM (gray traces) for the southern high-latitude passage (a) and the northern high-latitude passage (b). Arrows indicate the occurrence of the X-ray flares and CMEs in Table 1.

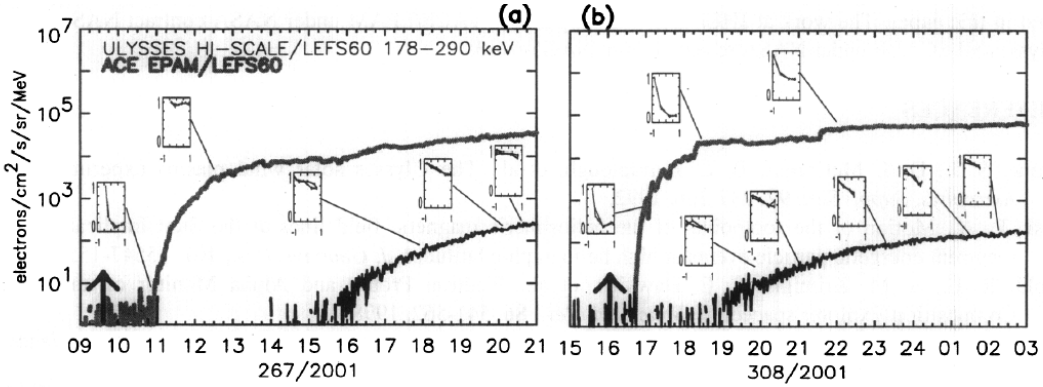

Fig. 3. 1-minute averages of 178-290 keV electron intensities as measured by HI-SCALE/LEFS60 (black traces) and EPAM/LEFS60 (gray traces) at the onset of events 1N (a) and 3N (b). Vertical arrows indicate the onset of the associated soft X-ray flare emission. Insets show the pitch-angle distributions for the 8 sectors of the detector LEFS60 in both instruments. Time units are in UT hours of the indicated day.

Motivation: solar wind heating

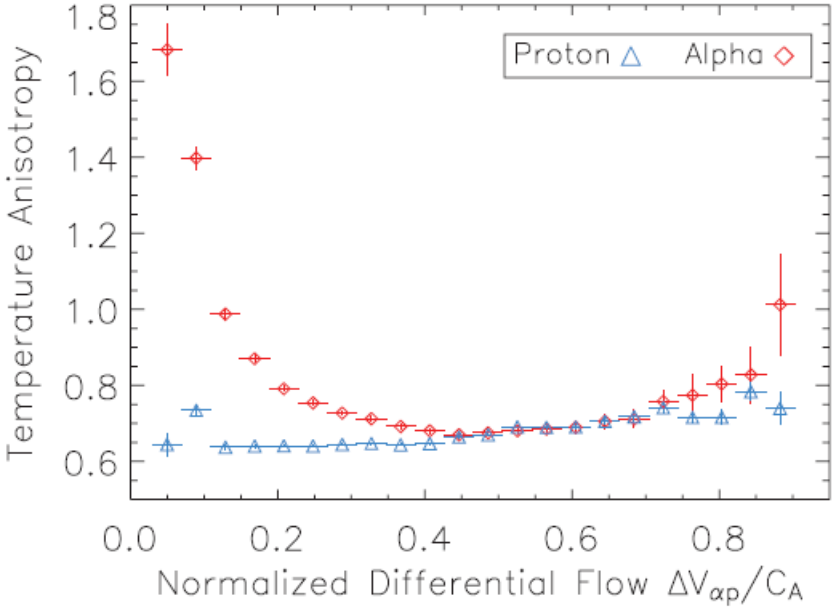

- J. C. Kasper *et al.*, Phys. Rev. Lett. **101**, 261103 (2008).
- Ion anisotropy $T_{\perp\alpha}/T_{\|\alpha}$, $T_{\perp p}/T_{\|p}$ in terms of $\triangle V_{\alpha p} \equiv V_\alpha - V_p$.

Favorable properties

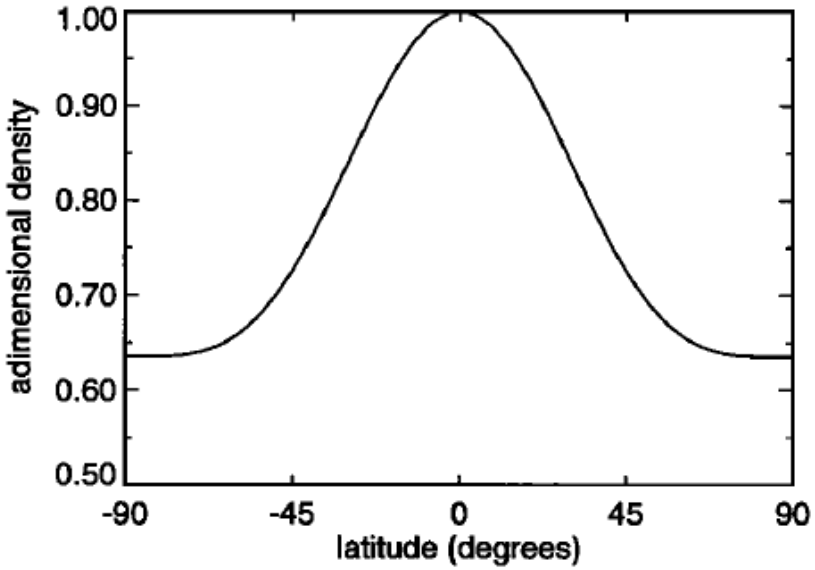

- J. Lima, K. Tsinganos, Geophys. Res. Lett. **23**, 117 (1996).
- Observations; the latitude dependent density in the solar wind.

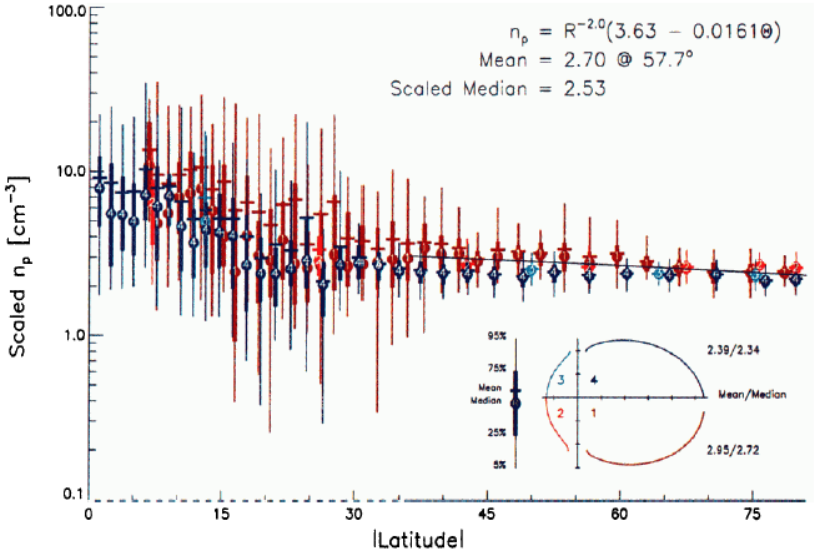

- D. J. McComas *et al.*, J. Geophys. Res. **105**(A5), 10419 (2000).
- Ulysses observations - the latitude dependent density in the solar wind.

Transverse drift wave in the corona

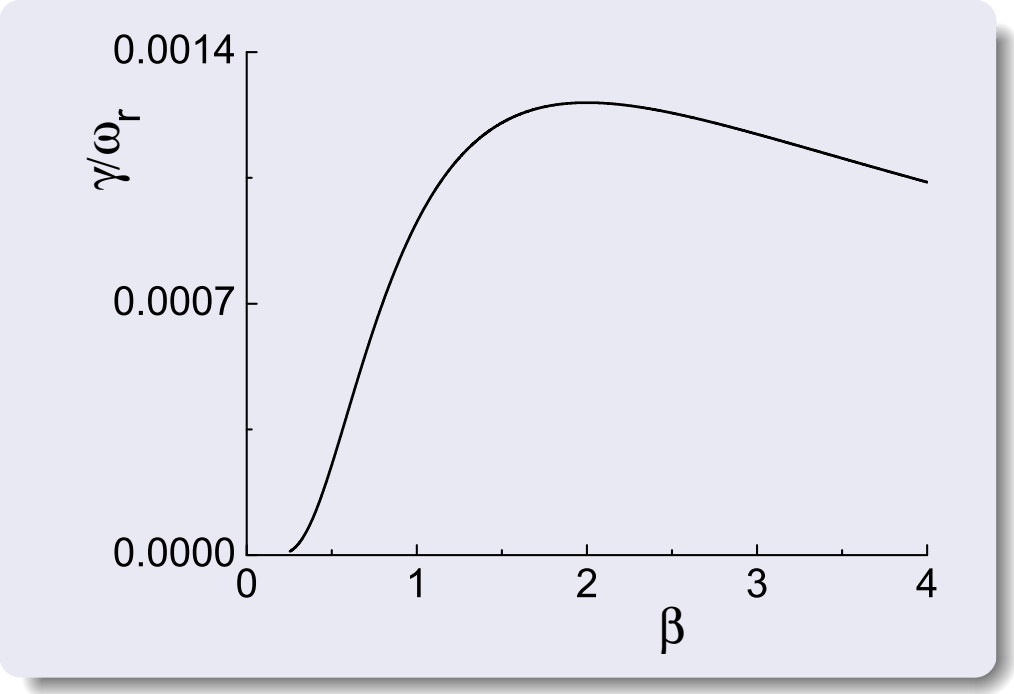

- J. Vranjes, Month. Not. Roy. Astron. Soc. **415**, 1543 (2011).
- Growth rate for coronal plasma parameters.
- $n_0 = 5 \cdot 10^{14}$ m^{-3}; $T_0 = 10^6$ K.
- For $\lambda_y = 100$ m, $L_n = 10^5$ m we have $\omega_r = 0.27$ Hz.
- For $L_n = 10^6$ m $\Rightarrow \omega_r = 0.027$ Hz.

- Acceleration: $v = (e\widehat{E}_1/m_i)\int_0^{\tau/2}\sin(\omega_r t) = 2e\widehat{E}_1/(m_i\omega_r)$; $\tau = 2\pi/\omega_r$.
- For $\widehat{E}_1 = 0.001$ V/m $\Rightarrow v = 700$ km/s; fast solar wind.
- For $\widehat{E}_1 = 0.02$ V/m $\Rightarrow$ MeV proton energy!

Used solar wind parameters

- At 1 AU:

$$T_i \simeq T_e = 1.5{\cdot}10^5 \ \text{K}, \quad n_{i0} = n_{e0} = n_0 = 5{\cdot}10^6 \ \text{m}^{-3}, \quad B_0 = 5{\cdot}10^{-9} \ \text{T},$$

$$L_n = 10^8 \ \text{m}, \quad \lambda = 10^6 \ \text{m}, \quad \text{plasma-beta} = 1.04, \quad \rho_i = 74 \cdot 10^3 \ \text{m},$$

$$\Omega_i \simeq 0.5 \ \text{Hz}, \quad \omega_r = 0.00016 \ \text{Hz}, \quad T_w \simeq 3.8 \cdot 10^4 \ \text{s}, [\simeq 10.7 \ \text{hours}]$$

- The ions are singly charged protons.
- Plasma magnetized; the local approximation well satisfied.
- The drift approximation $\omega_r/\Omega_i \ll 1$ well satisfied.
- Because $L_n/L_B = \beta/2 \Rightarrow L_b = 1.9 \cdot 10^8$ m.

$$\nu_{ii} = 1.4 \cdot 10^{-7} \, \text{Hz}, \quad \lambda_f = 2.6 \cdot 10^{11} \, \text{m}[\simeq 1.7 \ \text{AU!}]$$

- The classic perpendicular ion diffusion coefficient

$$D_\perp \approx \kappa T_i \nu_i / (m_i \Omega_i^2) = 736 \ \text{m}^2/\text{s}.$$

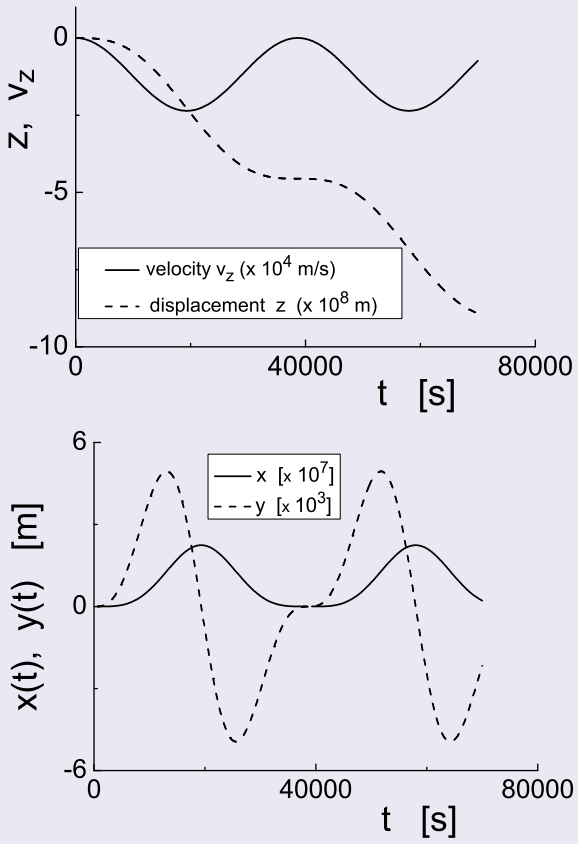

- J. Vranjes, Astron. Astrophys. **532**, A137 (2011).
- **Upper.** Full line: proton velocity along the magnetic field, in the wave field $\widehat{E}_{z1}\sin(-\omega t + ky)$ for $\widehat{E}_{z1} = 2 \cdot 10^{-8}$ V/m, $\omega_r = 0.00016$ Hz. Dashed line: the corresponding displacement along the magnetic field.
- The particle is subject to continuous directed drift along the magnetic field vector although the wave parallel electric field is oscillatory; around half million kilometers within one wave-period.
- **Lower.** The displacement in the x, y-plane, corresponding to the upper figure.

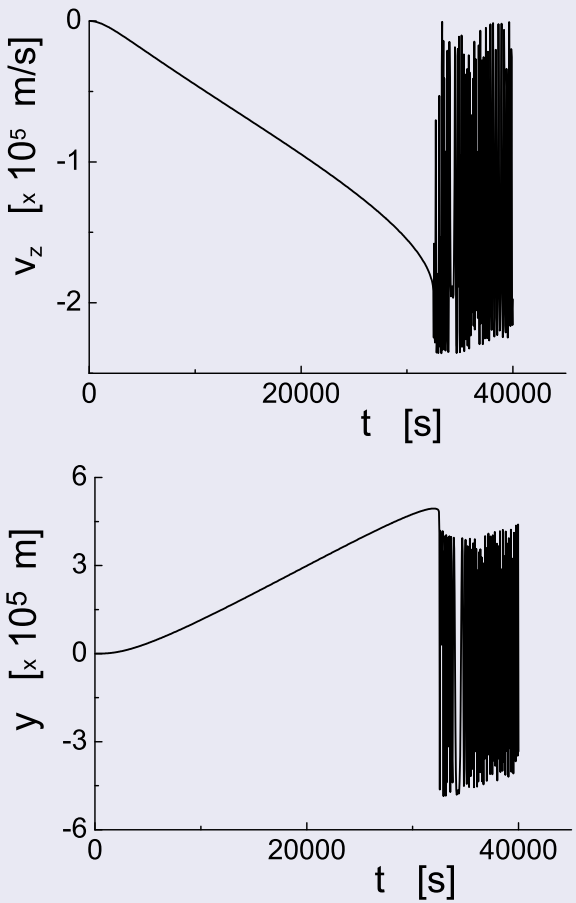

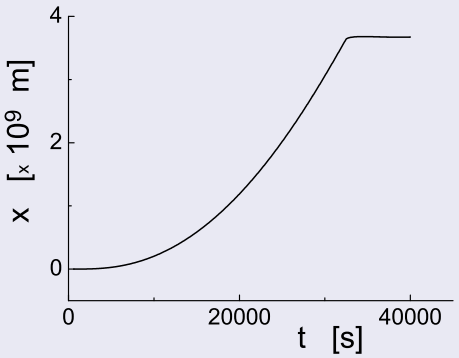

- Order of magnitude stronger electric field $\widehat{E}_{z1} = 2 \cdot 10^{-7}$ V/m.
- Stochastic motion develops after 8.9 hours.
- Displacement along the density gradient of the same order as the displacement in the z-direction. The x-displacement remains constant after the development of the stochastic motion. The particle already moved a few million kilometers. The average drift (diffusion) velocity is around $v_D = 1.2 \cdot 10^5$ m/s $\Rightarrow$ effective diffusion coefficient $D_\perp = v_D L_n = 1.2 \cdot 10^{13}$ m^2/s. [Note that this estimate is for the least favorable case, i.e., for the particles with zero starting velocity in the z-direction.]

- J. Vranjes, Astron. Astrophys. **532**, A137 (2011).

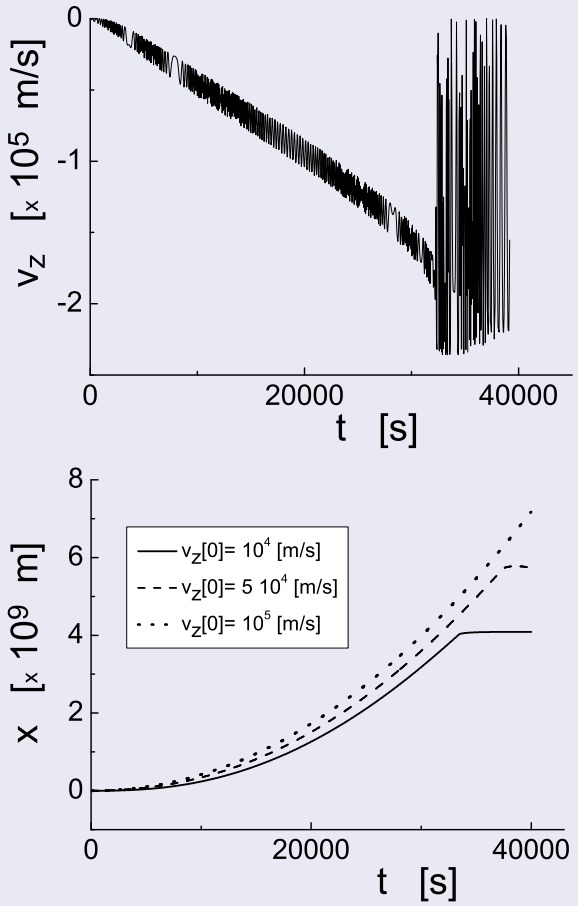

- J. Vranjes, Astron. Astrophys. **532**, A137 (2011).
- **Upper.** The velocity along the magnetic field vector for $v_y[0] = 10^4$ m/s.
- **Lower.** Drift perpendicular to the magnetic field, for three different starting velocities $v_z(0)$ in the direction of the background magnetic field.
  - A similar test done by taking $v_z(0) = 10^6$ m/s; within 19 hours the particle drifts to $x \simeq 3 \cdot 10^{10}$ m, i.e., to 0.2 AU.

New stochastic heating mechanism

- Follow two particles in the wave field; initially positions $\vec{r}_1, \vec{r}_2$; $\vec{r}_2 = \vec{r}_1 + \vec{\delta} r$; in general different velocities $\vec{v}_1, \vec{v}_2$:

$$\frac{d\vec{v}_1}{dt} = \frac{q}{m}\left[\vec{E}(\vec{r}_1, t) + \vec{v}_1 \times \vec{B}(\vec{r}_1, t)\right], \tag{21}$$

$$\frac{d\vec{v}_2}{dt} = \frac{q}{m}\left[\vec{E}(\vec{r}_2, t) + \vec{v}_2 \times \vec{B}(\vec{r}_2, t)\right]. \tag{22}$$

- Calculate the distance between the two.
- Subtracting them gives the displacement (forced harmonic oscillations due to the term on the right-hand side):

$$\frac{d^2\delta y}{dt^2} + \Omega^2\left[1 - \frac{v_{2,z}}{\Omega}\frac{\partial B_1(\vec{r}_1, t)/B_0}{\partial y}\right]\delta y = \Omega\frac{d\delta z}{dt}\frac{B_1(\vec{r}_1, t)}{B_0}. \tag{23}$$

- Introduced notation:

$$\vec{B}(\vec{r}_1,t)=\vec{B}_0+\vec{B}_1(\vec{r}_1,t),\quad \vec{B}(\vec{r}_2,t)=\vec{B}_0+\vec{B}_1(\vec{r}_1,t)+(\delta\vec{r}\cdot\nabla)\vec{B}_1(\vec{r}_1,t),$$

$$\vec{E}(\vec{r}_2,t)=\vec{E}_1(\vec{r}_1,t)+(\delta\vec{r}\cdot\nabla)\vec{E}_1(\vec{r}_1,t).$$

- The perpendicular distance δy between the two particles is determined by the parallel velocity of one of the particles.
- The distance can grow in time and this is equivalent to stochastic heating.
- Condition:

$$\delta\equiv\frac{v_{2,z}}{\Omega B_0}\frac{\partial B_1(\vec{r}_1,t)}{\partial y}>1. \tag{24}$$

- Some critical value for the parallel velocity $v_{2,z}$ is required!

- In the first approximation, from the parallel equation of motion $v_{2,z} = eE_{z1}/(m\omega_r)$

$$\delta \simeq \frac{k^2 \widehat{E}_{z1}^2}{\omega_r^2 B_0^2} > 1. \tag{25}$$

- The condition very easily satisfied, and, as a result, the particle motion in the wave field becomes stochastic for very small amplitude of the wave.
- In the given examples this happens for $\widehat{E}_{z1} \simeq 2 \cdot 10^{-7}$ V/m.
- Completely new stochastic heating mechanism.

Drift wave in solar plasma community

A letter from Editor

Dear Dr. Vranjes,
Re. XX-09-0376-XX - "The universally growing mode in the solar atmosphere: coronal heating by drift waves" by Vranjes, Poedts.

We have contacted **twelve potential reviewers** of your submission **so far without success.** If you wish to maintain your submission I would appreciate a list of at least six reviewers that you would consider competent to assess your submission.
My apologies for the delay, which neither I nor the editorial staff could have foreseen.

THANK YOU!

More details in:

- J. Vranjes and S. Poedts, A new pradigm for solar coronal heating, *Europhys. Lett.* **86**, 39001 (2009).
- J. Vranjes and S. Poedts, Solar nanoflares and smaller energy release events as growing drift waves, *Phys. Plasmas* **16**, 092902 (2009).
- J. Vranjes and S. Poedts, The universally growing mode in the solar atmosphere: coronal heating by drift wave, *MNRAS* **398**, 918 (2009).
- J. Vranjes and S. Poedts, Electric field in solar magnetic structures due to gradient driven instabilities: heating and acceleration of particles, *MNRAS* **400**, 2147 (2009).
- J. Vranjes and S. Poedts, Drift waves in the corona: heating and acceleration of ions at frequencies far below the gyro frequency, *MNRAS* **408**, 1835 (2010).
- J. Vranjes and S. Poedts, Kinetic instability of drift-Alfvén waves in solar corona and stochastic heating, *ApJ* **719**, 1335 (2010).
- J. Vranjes, Growing electric field parallel to magnetic filed due to transverse kinetic drift wave in inhomogeneous corona, MNRAS **415**, 1543 (2011).
- J. Vranjes, Transport and diffusion of particles in solar wind due to transverse drift wave, Astron. Astrophys. **532**, A137 (2011).

"I am not young enough to know everything" (Oscar Wilde).